

## RESEARCH ARTICLE OPEN ACCESS

# Malignant Rhabdoid Tumors of Cranial Nerves—A Clinically Distinct Group With Characteristic Neuroradiological, Histopathological, and Molecular Features

Miriam Gruhle<sup>1,2</sup> | Brigitte Bison<sup>2,3,4</sup> | Katharina Gastberger<sup>1,2</sup> | Pascal D. Johann<sup>1,2</sup> | Irene Teichert von Lüttichau<sup>2,5</sup> | Marc Steinborn<sup>6</sup> | Stephan Tippelt<sup>7</sup> | Gudrun Fleischhack<sup>7</sup> | Thomas Lehrnbecher<sup>8</sup> | Reiner Siebert<sup>9</sup> | Stefanie E. Tüchert-Knoll<sup>2,10</sup>  | Patrick Melchior<sup>11</sup> | Christian Vokuhl<sup>12</sup>  | Wolfgang Hartmann<sup>13</sup> | Martin Hasselblatt<sup>14</sup> | Michael C. Frühwald<sup>1,2</sup> 

<sup>1</sup>Pediatrics and Adolescent Medicine, University Hospital Augsburg, Swabian Children's Cancer Center, Augsburg, Germany | <sup>2</sup>Bavarian Cancer Research Center and KIONET, Augsburg, Germany | <sup>3</sup>Diagnostic and Interventional Neuroradiology, Faculty of Medicine, University Augsburg, Augsburg, Germany | <sup>4</sup>Neuroradiological Reference Center for the Pediatric Brain Tumor (HIT) Studies of the German Society of Pediatric Oncology and Hematology, Faculty of Medicine, University Augsburg, Augsburg, Germany | <sup>5</sup>Department of Pediatric Hematology/Oncology, Children's Hospital Medical Center, Technical University of Munich, Munich, Germany | <sup>6</sup>Department of Pediatric Radiology, München Klinik, Munich, Germany | <sup>7</sup>Department of Pediatric Hematology and Oncology, Pediatrics III, University Hospital of Essen, Essen, Germany | <sup>8</sup>Division of Hematology and Oncology, Department of Pediatrics, University Medicine, Goethe University Frankfurt, Frankfurt, Germany | <sup>9</sup>Institute of Human Genetics, Ulm University & Ulm University Medical Center, Ulm, Germany | <sup>10</sup>Department of Diagnostic and Interventional Radiology, University Medical Center Augsburg, Augsburg, Germany | <sup>11</sup>Department of Radiation Oncology, University of Saarland, Homburg, Germany | <sup>12</sup>Section of Pediatric Pathology, Department of Pathology, University Hospital Bonn, Bonn, Germany | <sup>13</sup>Gerhard Domagk Institute of Pathology, University Hospital Münster, Münster, Germany | <sup>14</sup>Institute of Neuropathology, University Hospital Münster, Münster, Germany

**Correspondence:** Michael C. Frühwald ([michael.fruehwald@uk-augsburg.de](mailto:michael.fruehwald@uk-augsburg.de))

**Received:** 7 April 2025 | **Revised:** 12 May 2025 | **Accepted:** 14 May 2025

**Funding:** This research was supported by the Deutsche Krebshilfe (Grant No. 70113981 and 70114040).

**Keywords:** atypical teratoid/rhabdoid tumor | cranial nerves | pediatric | schwannoma | SMARCB1

## ABSTRACT

**Background:** Malignant rhabdoid tumors occasionally develop along cranial nerves, but clinical, histopathological, and molecular features have not been examined in larger series.

**Procedure:** We retrospectively interrogated data from the European Rhabdoid Registry, EU-RHAB, to identify malignant rhabdoid tumors affecting cranial nerves. We retrieved clinical information and reviewed magnetic resonance imaging (MRI) data. Furthermore, histopathological review and molecular profiling were performed.

**Results:** Among 425 patients, we identified a total of 14 harboring malignant rhabdoid tumors with cranial nerve involvement. Median age at diagnosis was 28 months (range: 0–13 years). Various cranial nerves were affected, the trigeminal nerve ( $n = 4$ ) and the facial and/or vestibulocochlear nerve ( $n = 5$ ) being most frequently involved. In most cases, the initial clinical and neuroradiological suspicion was schwannoma. Neuroradiology review of magnetic resonance imaging studies confirmed a tumor

**Abbreviations:** AT/RT, atypical teratoid/rhabdoid tumor; MRT, malignant rhabdoid tumor; RTK, rhabdoid tumor of the kidney.

Martin Hasselblatt and Michael C. Frühwald contributed equally.

This is an open access article under the terms of the [Creative Commons Attribution](https://creativecommons.org/licenses/by/4.0/) License, which permits use, distribution and reproduction in any medium, provided the original work is properly cited.

© 2025 The Author(s). *Pediatric Blood & Cancer* published by Wiley Periodicals LLC.

along the cranial nerve, but signal characteristics with restricted diffusion were rather suggestive of a malignant tumor of high cellularity. Histopathological examination, using among others neurofilament staining confirmed the diagnosis and infiltration of nerve fascicles. DNA methylation profiles demonstrated high similarity with ATRT-MYC as well as extracranial malignant rhabdoid tumors (median calibrated scores: 1.00).

**Conclusions:** Malignant rhabdoid tumors of the cranial nerves represent a small but clinically distinct group, which initially is often not included in the differential diagnoses of pediatric cranial nerve tumors. Restricted diffusion on MRI may provide an early diagnostic clue. Histopathology and molecular signature are characteristic, but the developmental origin of malignant rhabdoid tumors of the cranial nerves remains to be determined.

## 1 | Introduction

Malignant rhabdoid tumors (MRT) are aggressive malignancies predominantly affecting children below 3 years of age, which are defined by mutations affecting *SMARCB1* or (rarely) *SMARCA4*, causing loss of protein expression of chromatin remodeling complex members *SMARCB1/INI1* or *SMARCA4/Brg1*, respectively [1]. Despite aggressive therapy, the outcome of many patients remains poor [2, 3]. Depending on anatomic location, MRT are classified as rhabdoid tumors of the central nervous system (atypical teratoid/rhabdoid tumor, AT/RT) [4], MRT of the kidney (RTK), and extrarenal MRT (eMRT) that may arise in various anatomic locations. Especially in spinal tumors, location of the bulk tumor within the intradural (denominated as AT/RT) or the extradural compartment (thus designated as eMRT) may be challenging and represents at best an arbitrary classification. There is consensus that AT/RT comprises at least three distinct molecular groups characterized by DNA methylation profiles and gene expression signatures [5]. ATRT-MYC represents the molecular group with the lowest incidence, is characterized by MYC activation [6], and shares similarities with extracranial MRT [6]. Cases of malignant rhabdoid tumors affecting cranial nerves are on record [7–11], but clinical and neuropathological features have thus far not been systematically examined in larger series.

Here, we demonstrate that MRT of the cranial nerves represent a small but clinically distinct group of tumors with characteristic neuroradiological, histopathological, and molecular features.

## 2 | Methods

We screened the database of the European Rhabdoid Registry (EU-RHAB), comprising 425 patients harboring MRT of all anatomical locations (February 2010 to March 2022) for tumors with cranial nerve involvement. This reference cohort included 282 patients with AT/RT, 121 patients with MRT, as well as 22 patients with synchronous rhabdoid tumors (AT/RT in combination with either MRT of the kidney [ $n = 7$ ] or extrarenal MRT [ $n = 15$ ], respectively). Magnetic resonance imaging studies of these cases were centrally reviewed. Whenever (on MRI) tumors apparently grew along the course of the respective cranial nerves or when the major tumor mass was located right on the nerve or at least closer to the nerve than to any other nervous tissue in the proximity, the tumor was considered a tumor of the cranial nerve. Clinical information

regarding symptoms at presentation, therapeutic approaches, and outcome was compiled from the EU-RHAB database. Local surgical reports were reviewed and provided information on the macroscopic description of the tumor upon surgery. Histopathological review of tumor tissues was performed according to current WHO criteria. In addition, immunohistochemistry for neurofilament and SOX10 was executed on an automated staining machine (DAKO Omnis, Agilent). Genetic analyses included fluorescence in situ hybridization, multiplex ligation-dependent probe amplification (MRC-Holland, Kit-P258-C1/-C2), OncoScan (OncoScan Affymetrix, Software ChAS 4.0/4.2), as well as next-generation sequencing (NGS; Illumina MiSeq, MiSeq Reagent Kit v.3 Flow Cell). DNA methylation profiles were generated using Human Methylation 450 BeadChip arrays (Cases #8 and #14) or Methylation EPIC BeadChip arrays (Illumina Inc., San Diego, CA) and analyzed using the central nervous system tumor classifier (Version 12.8) as well as the sarcoma classifier (Version 12.3, DKFZ Heidelberg, <https://www.moleculareuropathology.org>) [12, 13]. We obtained written consent for data acquisition from all patients' legal guardians. Ethics committee approval of the EU-RHAB registry has been granted continuously since 2010 (ID 2009-532-f-S, last amendment 2021).

## 3 | Results

Among the cohort of 425 patients with MRT of all anatomical locations, 14 patients (3%) harboring cranial nerve involvement were identified. These included five male and nine female patients with a median age at diagnosis of 28 months (range: 0–13 years) (Table 1). Various cranial nerves were affected, the trigeminal nerve ( $n = 4$ ) and the vestibulocochlear and the facial nerve ( $n = 5$ ) being most frequently involved. In three cases, the oculomotor nerve and in one case the abducens and hypoglossal nerve were affected. Due to the close anatomical proximity of the facial and the vestibulocochlear nerves, it was not possible to define the nerve of origin as the tumor included the course of both at the time of diagnosis. As no tumor reached the facial canal, a vestibulocochlear origin is more likely in these cases. Location of the bulk tumor was either intradural in nine cases (64%) or extradural in five cases, which subsequently had either prompted the initial histopathological diagnosis of AT/RT (intradural, central nervous system [CNS] location) or MRT (extradural, non-CNS location), respectively. Metastases at diagnosis were visible on MRI in five patients (36%), and in four additional patients on follow-up. None of the 14 patients harbored synchronous MRT in other locations (Table 2).

**TABLE 1** | Patient characteristics in 14 children with cranial nerve eMRT.

ID2#	m/f	time to initial MRI (months)	Symptoms at presentation	Anatomic location	Cranial nerve	Side	Tentative clinical diagnosis
1	m	3	Proptosis, oculomotor nerve palsy	Intraorbital, cavernous sinus	Oculomotor nerve	Right	Rhabdomyosarcoma
2	f	1	Oculomotor nerve palsy	Cisternal course	Oculomotor nerve	Right	High-grade glioma vs. AT/RT
3	m	5	Oculomotor nerve palsy	Cisternal course, reaching the temporal lobe	Oculomotor nerve	Left	Schwannoma
4	f	61	Abducens nerve palsy	Cisternal course/Meckel cave/oval foramen/infratemporal fossa	Trigeminal nerve	Left	Schwannoma
5	f	8	Vomiting	cisternal course/Meckel cave/infratemporal fossa	Trigeminal nerve	Right	Rhabdomyosarcoma
6	f	39	Ataxia	CPA/IAC	Vestibulocochlear/facial nerve	Left	Schwannoma
7	f	23	Facial pain, ptosis	Meckel cave, infratemporal fossa	Trigeminal nerve	Right	Unknown
8	m	158	Headache, facial hemihypoesthesia	Cisternal course/Meckel cave/oval foramen/infratemporal fossa	Trigeminal nerve	Left	Nerve sheath tumor
9	f	19	Abducens nerve palsy	Cisternal course/Dorello canal	Abducens nerve	Left	Abscess
10	m	79	Facial nerve palsy	CPA/IAC	Vestibulocochlear/facial nerve	Right	Vestibular schwannoma
11	m	6	Facial nerve palsy	CPA/IAC	Vestibulocochlear/facial nerve	Left	Vestibular schwannoma
12	f	48	Facial nerve palsy, hearing impairment	CPA/IAC	Vestibulocochlear/facial nerve	Right	Anaplastic astrocytoma
13	f	55	Facial nerve palsy	CPA/IAC/infiltration of petrous bone	Vestibulocochlear/facial nerve	Right	Schwannoma
14	f	34	Headache, vomiting, nuchal rigidity	CPA/hypoglossal canal	Hypoglossal nerve	Right	Unknown

Abbreviations: CPA, cerebellum-pontine angle; eMRI, extracranial magnetic resonance imaging; IAC, internal auditory canal.

TABLE 2 | Differentiation of rhabdoid tumors derived from cranial nerves vs. schwannoma vs. meningioma.

Case	Schwannoma imaging Features of schwannoma	Features unlike schwannoma	Meningeoma imaging Features of meningioma	Features unlike meningioma	Possible rhabdoid tumor Typical for AT/TR
1	Along course of cranial nerve	Round, not spindle-shaped, hypoglossal canal	None	No MO	Hypoglossal canal
2	Along course of cranial nerve	Round, not spindle-shaped, no demarcation, M+	None	No MO, M+	Hypoglossal canal, M+
3	Along course of cranial nerve	Round, irregular, not spindle-shaped, no demarcation, M+	None	No MO, M+	Hypoglossal canal, no demarcation, M+
4	Along course of cranial nerve	Round, not dumbbell-shaped	Yes, along CS, small MT	Thickening along nerve	Hypoglossal canal
5	Along course of cranial nerve	Round, not dumbbell-shaped	None	Thickening along nerve	Hypoglossal canal
6	Along course of cranial nerve, small part reaching into IAC, BR	Round, not ICC-shaped, BR unremarkable, M+	Yes, broad-based along PB	Too "round", no MT, M+	Hypoglossal canal, M+
7	Along course of cranial nerve	Round, not dumbbell-shaped	None	No MO	Hypoglossal canal
8	Along course of cranial nerve	Not dumbbell-shaped	None	Too "round", little MC, no MT, M+	Hypoglossal canal
9	Along course of cranial nerve	Round, no demarcation, M+	None	Little MC	Hypoglossal canal, M+
10	Along course of cranial nerve	Round, not ICC-shaped, no demarcation, M+	Broad along PB, MT	"Round," BR	Hypoglossal canal, M+
11	Along course of cranial nerve, BR of IAC	Not ICC-shaped	None	Little MC	Hypoglossal canal
12	Along course of cranial nerve, BR of IAC	Not ICC-shaped	Yes, broad-based along PB	Hypoglossal canal, BR	Hypoglossal canal
13	Along course of cranial nerve, BR of IAC	Bone destruction	Broad-based along PB, MT	None	Hypoglossal canal, BD
14	Along course of cranial nerve, BR of HC	round, M+	Broad-based along PB, MT	None	Hypoglossal canal, M+

Note: "round": in contrast to the typical "spindle-shaped" appearance of a schwannoma. "dumbbell-shaped": typical impression of schwannoma tissue elicited by the tumor's passage through the dura located at Meckel's cave. "ice cream on cone" (ICC): typical configuration of schwannoma with significantly widened IAC and round tumor in the cerebellopontine angle. Abbreviations: BD, bone destruction; BR, bone remodeling; CS, cavernous sinus; HC, hypoglossal canal; IAC, internal auditory canal; MO, meningeal origin; MC, meningeal contact; MT, meningioma tails; M+, dissemination; PB, petrous bone.

### 3.1 | Symptoms at Presentation

In most cases (10/14, 86%), symptoms at presentation were related to disturbed function of the affected cranial nerves such as facial palsy, ptosis, abducens palsy, one-sided facial pain or hypoesthesia. Other non-specific symptoms included headaches, ataxia, vomiting, refusal to walk, and signs of local pressure (e.g., protrusion of the eyeball). In most cases, cranial nerve symptoms led to an initial clinical working diagnosis of schwannoma. Other initial diagnoses comprised rhabdomyosarcoma or, misguided by the restricted diffusion, an intracranial abscess. Only two patients had initially been classified as highly malignant tumors with cranial nerve involvement (one case as AT/RT and another as malignant glioma).

### 3.2 | Magnetic Resonance Imaging Features

Neuroradiology findings had initially often been reported as suggestive of nerve sheath tumor (8/14) or rhabdomyosarcoma (3/14). Highly malignant tumors had only been considered in two cases. On central neuroradiology review, all cases demonstrated MRI signal characteristics meeting previously described criteria of rhabdoid tumors [14, 15]. These included predominant iso- to hypointensity on T2-weighted sequences, heterogeneous contrast enhancement of mild to intermediate intensity, in contrast to the strong enhancement typically demonstrated in schwannoma, and restricted diffusion with low acquired diffusion coefficient (ADC) when compared to normal brain as an imaging correlate of high cellularity. In contrast to schwannomas, which characteristically demonstrate a spindle-shaped configuration, most cases were rather round with an expansive character. The trigeminal nerve tumors did not demonstrate the typical constriction when passing through the trigeminal porus, usually referred to as “dumbbell-shaped” (Figure 1). In cases of vestibulocochlear and facial involvement, the lesions did not show the typical “ice cream on cone” appearance, with a conical part widening the internal auditory canal and a spherical part reaching into the cerebellopontine angle [16]. Here, we saw uniformly spindle-shaped tumors on one side as well as those with large broad-based parts along the petrous bone resembling meningiomas with a typical dural tail. In one case, in which a computer tomography was available, osseous destruction was visible (Figure 2, Table 2, Table S1). All tumors apparently originated from the corresponding nerve and represented the largest tumor mass occurring along the course of the nerve, even when considering M+ lesions. M+ lesions were exclusively leptomeningeal.

### 3.3 | Histopathological Features

On histopathological examination, highly malignant cellular tumors with typical rhabdoid features were encountered (Figure 3). All tumors demonstrated complete loss of nuclear SMARCB1/INI1 staining. There were no SMARCA4-deficient cases. Importantly, we observed no histopathological difference between cases that had initially received a diagnosis of AT/RT (exclusive or predominant location within the CNS) or MRT (predominantly non-CNS location), and many cases showed morphological patterns typically encountered in ATRT-MYC [17], that is, a predominant mesenchymal or rhabdoid phenotype. In

six cases, for which material for additional immunohistochemical studies was available, neurofilament staining was performed and highlighted tumor infiltration of nerve fascicles in all cases examined. Tumor cells stained negative for SOX10.

### 3.4 | Molecular Genetics

Molecular genetic examination of tumor tissues revealed *SMARCB1* alterations in all cases, including homozygous deletions of *SMARCB1* ( $n = 5$ ), heterozygous *SMARCB1* deletions ( $n = 5$ ), and *SMARCB1* duplications ( $n = 2$ ), as well as various truncating *SMARCB1* point mutations and indels (for details see Table S1). Germline pathogenic *SMARCB1* variants were discovered in three out of 13 patients, for which information on germline *SMARCB1* status was available (23%). DNA methylation profiling was performed in 10 cases. All these tumors were clearly classified as ATRT-MYC using the CNS tumor classifier (Version 12.8, median calibrated score: 1.00), but notably also as MRT using the sarcoma classifier (Version 12.3, median calibrated score: 1.00).

### 3.5 | Therapeutic Approaches and Clinical Outcome

Gross tumor resection was achieved in only one patient, who consecutively experienced loss of nerve function. Four patients achieved complete remission at some point. Chemotherapy according to a consensus regimen [18, 19] was administered in 11 cases with different numbers of courses (3–12). Therapy was enhanced by intraventricular methotrexate ( $n = 10$ ) or high-dose chemotherapy ( $n = 1$ ). Nine patients received radiotherapy. Mean overall survival was 1.93 (0.11–11.79) years. Survival at 1 and 2 years was 50% and 35.7%, respectively. Of note, all five patients who were alive at the time of this report had received radiotherapy.

## 4 | Discussion

The current cohort represents the largest series of patients with MRT affecting cranial nerves reported thus far. Our findings demonstrate that this distinct clinical group is often overlooked in the initial differential diagnosis of pediatric tumors involving the cranial nerves. This study highlights the epigenetic similarity of these cases to ATRT-MYC and extrarenal MRT.

In comparison to previously reported cases of MRT with cranial nerve involvement [7–11], the spectrum of cranial nerves affected by tumor growth is wider, including a remarkable case originating from the hypoglossal nerve. As clinical signs and symptoms are similar to cranial nerve schwannomas, knowledge about their incidence in young children, especially in those without a predisposition such as neurofibromatosis type 2, and of magnetic resonance imaging characteristics of MRT with cranial nerve involvement is essential for a timely diagnosis. Both tumor entities exhibit the same localization and extension along the cranial nerves, but schwannomas in general demonstrate signs of low cellularity, sometimes accompanied by necroses and cysts. They display a low signal on T1-weighted images, but a high

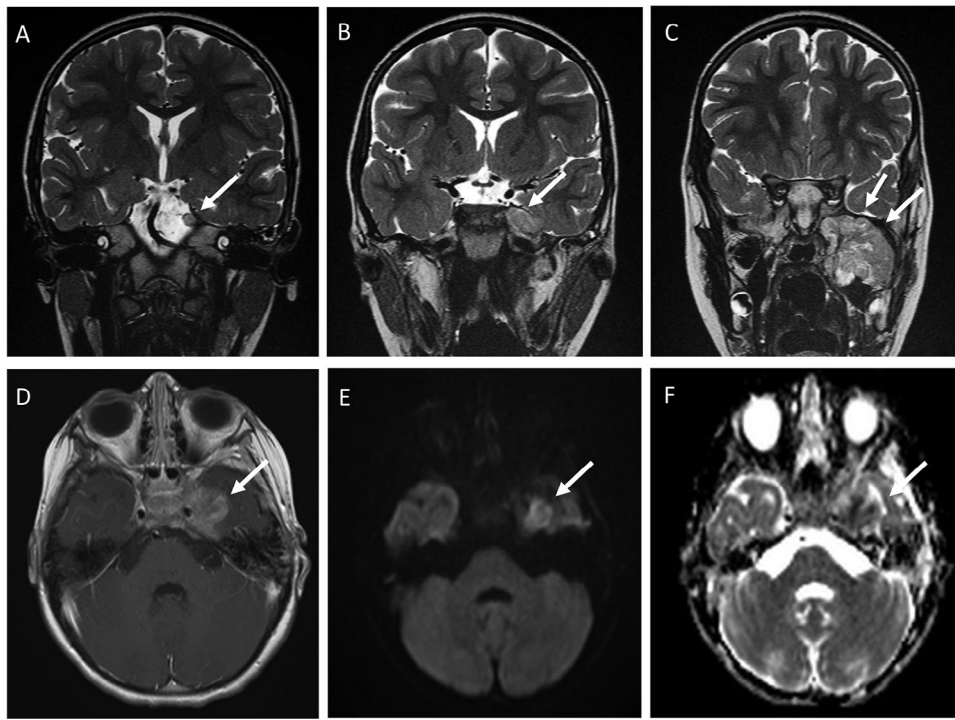


**FIGURE 1** | Magnetic resonance imaging (MRI) of a rhabdoid tumor of the trigeminal nerve. This 5-year-old female developed palsy of the left-sided abducens nerve. MRI revealed a tumor growing along the trigeminal nerve. The upper row shows coronal T2-weighted images: a small cysternal part (A, arrow), in the cave of Meckel (B, arrow), and with expansion through the oval foramen, the mandibular branch building the predominant part of the tumor extracranially in the infratemporal fossa (C, arrows). The lower row shows the axial plane at the level of the widened cave of Meckel. T1-weighted image following contrast application with enhancement of intermediate intensity (D, arrows), and on diffusion-weighted images, a very bright signal on b1000 (E, arrow) and very low acquired diffusion coefficient (F, arrow). The bulk of the tumor is in the extradural space. All neuroradiology images were independently reviewed by at least one independent neuroradiologist of the reference center for neuroradiology of the German HIT-network for CNS tumors.

signal intensity on T2-weighted images and a strong contrast enhancement of the solid part. AT/RT and the predominantly extradural MRT demonstrate imaging criteria of high cellularity, they exhibit an intermediate to low signal on T2-weighted images, and in most cases, intermediate to mild intensity of contrast enhancement. They do not display the typical configuration of schwannomas with “ice cream on cone” or “dumbbell” appearance can be ill-defined and infiltrative in some parts and may display bone infiltration. For the distinction of schwannomas and MRT of the cranial nerve, the most sensitive sequence on MRI is diffusion-weighted imaging. Our study confirms that restricted diffusion is a characteristic finding of high cellularity and is the method of choice to diagnose MRT of the cranial nerves [9]. It allows for the distinction from benign schwannomas, which usually display increased diffusibility, consistent with high ADC values [20].

By contrast, malignant peripheral nerve sheath tumors demonstrate peritumoral edema, hemorrhage, and/or necrosis, as well as heterogeneous contrast enhancement but also restricted diffusion [20], and are thus difficult to distinguish from MRT by neuroradiology techniques only. However, intracranial malignant peripheral nerve sheath tumors are extremely rare and represent an exceptional finding in children. Furthermore, such rare cases typically demonstrate characteristic clinical features of neurofibromatosis type 1 or 2 [21]. This also applies to the differential diagnosis of meningioma, which is extremely rare in this age

group and also occurs in the context of neurofibromatosis type 2 [22]. Even though the tumor location of MRT of the cranial nerves is comparable to that of intracranial schwannomas, young age and the absence of a component with retained SMARCB1 staining argue against the secondary development of MRT from a pre-existing schwannoma. Furthermore, in other tumor types that may develop a secondary MRT component, such as pleomorphic xanthoastrocytoma, the secondary MRT component usually retains genetic and epigenetic features of the pre-existing tumor [23].

The cellular origin of MRT of cranial nerves remains elusive. The epigenetic similarity of the DNA methylation profiles of ATRT-MYC and extrarenal MRT [6] is intriguing and suggests a common cell of origin. Indeed, work comparing bulk gene expression profiles from AT/RT to that of single-cell RNAseq data of the developing mouse brain suggests a non-CNS origin of ATRT-MYC [24]. Such cells of origin might well represent a Schwann cell precursor, which acquires biallelic SMARCB1 mutations during an early phase of development. Of note, the vast majority of spinal AT/RT also belong to the ATRT-MYC group and frequently affect spinal nerve roots [5, 25, 26]. The absent histopathological evidence for Schwann cell differentiation (including absent expression of the Schwann cell marker SOX10) in MRT of the cranial nerves, as in extracranial MRT in general [27], could be well related to the profound effects of SMARCB1 loss on proliferation and differentiation [28–30].

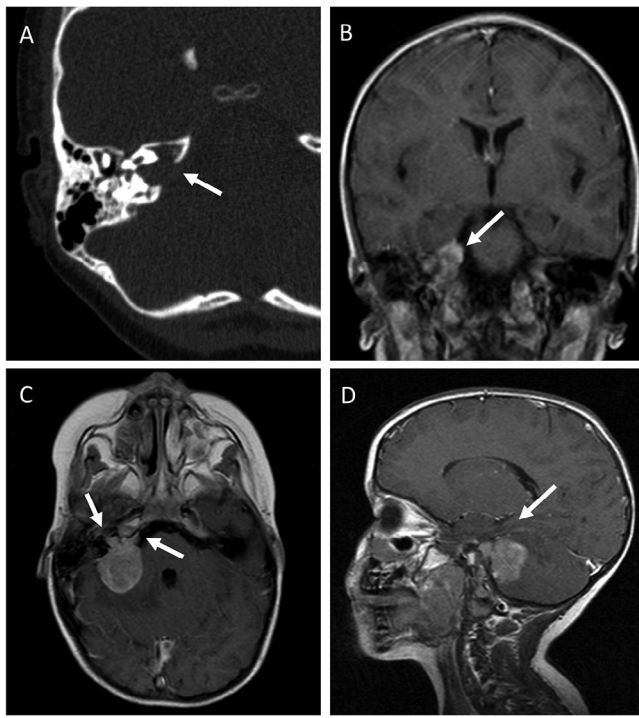


**FIGURE 2** | Computed tomography and magnetic resonance imaging of a rhabdoid tumor of the facial nerve. The 4-year-old female suffered from facial nerve palsy. The computed tomography (A, axial plane, bone reconstruction) demonstrates some bone destruction (arrow), the T1-weighted contrast-enhanced images (B, coronal plane; C, axial plane; D, sagittal plane) demonstrate the tumor with the predominant part in the cerebellopontine angle. In contrast to the typical “ice cream on cone” appearance of a schwannoma, the tumor is broadly based along the petrous bone with “meningioma tails” (C, arrow) and displays contrast enhancement of intermediate intensity. There are no necroses as commonly seen in schwannomas of this size.

The vast majority of MRT of the cranial nerves was encountered in infants, among them a proportion of cases with rhabdoid tumor predisposition syndrome 1 (OMIM #609322), suggesting that (as in MRT of other locations and AT/RT) inactivation of *SMARCB1* alone is sufficient for the development of MRT of the cranial nerves. In contrast, *SMARCB1*-negative schwannomas in familial schwannomatosis (OMIM# 162091) are mainly encountered in older children and adults [31], and tumors often carry somatic alterations of *SMARCB1* and *NF2*, suggesting a four-hit mechanism [32, 33]. Furthermore, the mutational spectrum is different, schwannomas in familial schwannomatosis often demonstrate N-terminal and/or non-truncating *SMARCB1* mutations [34], and mechanisms such as translational reinitiation may result in altered *SMARCB1* proteins with modified activity [35]. In some families with germline *SMARCB1* alterations, the co-occurrence of malignant rhabdoid tumors in children as well as schwannomatosis in adults links rhabdoid tumor predisposition syndrome and schwannomatosis [36]. Experimental data in mouse models suggest that the timing of *Smarchb1* and *Nf2* inactivation determines schwannoma versus rhabdoid tumor development [37].

Our current series is retrospective, and outcome data need interpretation with caution. Nevertheless, our data suggest that

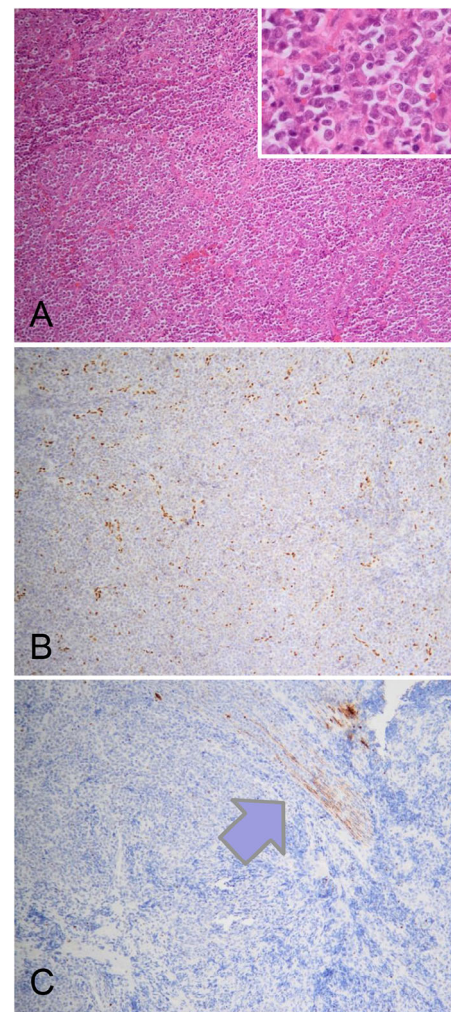


**FIGURE 3** | Histopathology (Case 6). The female patient presented with ataxia at the age of 2 years. The tumor was resected. On histopathological examination (A), a highly cellular tumor composed of rhabdoid tumor cells with prominent nucleoli and/or eosinophilic inclusions (inset) was encountered. Tumor cells show loss of nuclear *SMARCB1/INI1* expression (B), which is retained in non-neoplastic nuclei (internal positive control). Neurofilament staining (C) further highlights infiltration of nerve fascicles (arrow).

the overall survival of children with MRT of the cranial nerves is rather unfavorable and thus comparable to children harboring AT/RT of the molecular group ATRT-MYC [18] and extracranial MRT in general [19]. The fact that all surviving patients harboring MRT of the cranial nerves had received radiotherapy as part of their primary management is in line with a beneficial prognostic role of radiotherapy in extracranial MRT [19], but warrants further examination within prospective trials.

## 5 | Conclusions

Malignant rhabdoid tumors of the cranial nerves constitute a small but distinct clinically defined group that is often overlooked in the initial diagnosis of pediatric cranial nerve tumors. Clinicians should consider this diagnosis, particularly in young children, when atypical features or signs of tumor spread are

present. Standardized diagnostic imaging following established guidelines, including diffusion-weighted imaging, is essential [38]. Restricted diffusion on magnetic resonance imaging can offer an early diagnostic clue. While the histopathology and molecular signature are characteristic, the exact origin of these tumors remains to be determined.

### Acknowledgments

M.C.F.'s work on rhabdoid tumors is supported by the Deutsche Kinderkrebsstiftung. M.C.F. and R.S. received support by the Deutsche Krebshilfe (Grant No. 70113981 and 70114040).

Open access funding enabled and organized by Projekt DEAL.

### Conflicts of Interest

The authors declare no conflicts of interest.

### References

1. K. Kerl, T. Holsten, and M. C. Frühwald, "Rhabdoid Tumors: Clinical Approaches and Molecular Targets for Innovative Therapy," *Pediatric Hematology and Oncology* 30, no. 7 (2013): 587–604.
2. K. Nemes, P. D. Johann, S. Tuchert, et al., "Current and Emerging Therapeutic Approaches for Extracranial Malignant Rhabdoid Tumors," *Cancer Management and Research* 14 (2022): 479–498.
3. K. Gastberger, V. E. Fincke, M. Mucha, R. Siebert, M. Hasselblatt, and M. C. Frühwald, "Current Molecular and Clinical Landscape of ATRT—The Link to Future Therapies," *Cancer Management and Research* 15 (2023): 1369–1393.
4. L. B. Rorke, R. J. Packer, and J. A. Biegel, "Central Nervous System atypical Teratoid/Rhabdoid Tumors of Infancy and Childhood: Definition of an Entity," *Journal of Neurosurgery* 85, no. 1 (1996): 56–65.
5. B. Ho, P. D. Johann, Y. Grabovska, et al., "Molecular Subgrouping of atypical Teratoid/Rhabdoid Tumors—A Reinvestigation and Current Consensus," *Neuro-Oncology* 22, no. 5 (2020): 613–624.
6. H. E. Chun, P. D. Johann, K. Milne, et al., "Identification and Analyses of Extra-Cranial and Cranial Rhabdoid Tumor Molecular Subgroups Reveal Tumors With Cytotoxic T Cell Infiltration," *Cell Reports* 29, no. 8 (2019): 2338–2354.e7.
7. C. C. Wykoff, B. L. Lam, C. D. Brathwaite, et al., "Atypical Teratoid/Rhabdoid Tumor Arising From the Third Cranial Nerve," *Journal of Neuro-Ophthalmology* 28, no. 3 (2008): 207–211.
8. A. Siu, M. Lee, R. Rice, and J. S. Myseros, "Association of Cerebellopontine Angle atypical Teratoid/Rhabdoid Tumors With Acute Facial Nerve Palsy in Infants," *Journal of Neurosurgery* 13, no. 1 (2014): 29–32.
9. J. S. Katz, P. P. Peruzzi, C. R. Pierson, J. L. Finlay, and J. R. Leonard, "Cerebellopontine Angle Tumors in Young Children, Displaying Cranial Nerve Deficits, and Restricted Diffusion on Diffusion-Weighted Imaging: A New Clinical Triad for atypical Teratoid/Rhabdoid Tumors," *Child's Nervous System* 33, no. 5 (2017): 833–838.
10. D. Rizzo, P. Freneaux, H. Brisse, et al., "SMARCB1 Deficiency in Tumors From the Peripheral Nervous System: A Link Between Schwannomas and Rhabdoid Tumors?," *American Journal of Surgical Pathology* 36, no. 7 (2012): 964–972.
11. C. C. Oh, B. A. Orr, B. Bernardi, et al., "Atypical Teratoid/Rhabdoid Tumor (ATRT) Arising From the 3rd Cranial Nerve in Infants: A Clinical-Radiological Entity?," *Journal of Neuro-Oncology* 124, no. 2 (2015): 175–183.
12. D. Capper, D. T. W. Jones, M. Sill, et al., "DNA Methylation-Based Classification of central Nervous System Tumours," *Nature* 555, no. 7697 (2018): 469–474.
13. C. Koelsche, D. Schrimpf, D. Stichel, et al., "Sarcoma Classification by DNA Methylation Profiling," *Nature Communications* 12, no. 1 (2021): 498.
14. K. Koral, L. Gargan, D. C. Bowers, et al., "Imaging Characteristics of Atypical Teratoid-Rhabdoid Tumor in Children Compared With Medulloblastoma," *Ajr American Journal of Roentgenology* 190, no. 3 (2008): 809–814.
15. M. Warmuth-Metz, B. Bison, E. Dannemann-Stern, R. Kortmann, S. Rutkowski, and T. Pietsch, "CT and MR Imaging in Atypical Teratoid/Rhabdoid Tumors of the central Nervous System," *Neuroradiology* 50, no. 5 (2008): 447–452.
16. A. G. Osborn, *Osborn's Brain* (Elsevier, 2018).
17. F. Zin, J. A. Cotter, C. Haberler, et al., "Histopathological Patterns in atypical Teratoid/Rhabdoid Tumors Are Related to Molecular Subgroup," *Brain Pathology* 31, no. 5 (2021): e12967.
18. M. C. Frühwald, M. Hasselblatt, K. Nemes, et al., "Age and DNA Methylation Subgroup as Potential Independent Risk Factors for Treatment Stratification in Children With Atypical Teratoid/Rhabdoid Tumors," *Neuro-Oncology* 22, no. 7 (2020): 1006–1017.
19. K. Nemes, S. Bens, D. Kachanov, et al., "Clinical and Genetic Risk Factors Define Two Risk Groups of Extracranial Malignant Rhabdoid Tumours (eMRT/RTK)," *European Journal of Cancer* 142 (2021): 112–122.
20. A. T. Mazal, O. Ashikyan, J. Cheng, L. Q. Le, and A. Chhabra, "Diffusion-Weighted Imaging and Diffusion Tensor Imaging as Adjuncts to Conventional MRI for the Diagnosis and Management of Peripheral Nerve Sheath Tumors: Current Perspectives and Future Directions," *European Radiology* 29, no. 8 (2019): 4123–4132.
21. C. Newell, A. Chalil, K. D. Langdon, et al., "Cranial Nerve and Intramedullary Spinal Malignant Peripheral Nerve Sheath Tumor Associated With Neurofibromatosis-1," *Surgical Neurology International* 12 (2021): 630.
22. K. Wagener, J. Beckhaus, S. Boekhoff, C. Friedrich, and H. L. Müller, "Sporadic and Neurofibromatosis Type 2-Associated Meningioma in Children and Adolescents," *Journal of Neuro-Oncology* 163, no. 3 (2023): 555–563.
23. C. Thomas, A. Federico, M. Sill, et al., "Atypical Teratoid/Rhabdoid Tumor (AT/RT) with Molecular Features of Pleomorphic Xanthoastrocytoma," *American Journal of Surgical Pathology* 45, no. 9 (2021): 1228–1234.
24. S. Jessa, A. Blanchet-Cohen, B. Krug, et al., "Stalled Developmental Programs at the Root of Pediatric Brain Tumors," *Nature Genetics* 51, no. 12 (2019): 1702–1713.
25. P. D. Johann, S. Erkek, M. Zapatka, et al., "Atypical Teratoid/Rhabdoid Tumors Are Comprised of Three Epigenetic Subgroups With Distinct Enhancer Landscapes," *Cancer Cell* 29, no. 3 (2016): 379–393.
26. M. Benesch, K. Nemes, P. Neumayer, et al., "Spinal Cord atypical Teratoid/Rhabdoid Tumors in Children: Clinical, Genetic, and Outcome Characteristics in a Representative European Cohort," *Pediatric Blood & Cancer* 67, no. 1 (2020): e28022.
27. S. Gadd, S. T. Sredni, C. C. Huang, and E. J. Perlman, "Renal Tumor Committee of the Children's Oncology G. Rhabdoid Tumor: Gene Expression Clues to Pathogenesis and Potential Therapeutic Targets," *Laboratory Investigation* 90, no. 5 (2010): 724–738.
28. I. Versteeg, S. Medjkane, D. Rouillard, and O. Delattre, "A Key Role of the hSNF5/INI1 Tumour Suppressor in the Control of the G1-S Transition of the Cell Cycle," *Oncogene* 21, no. 42 (2002): 6403–6412.
29. M. S. Isakoff, C. G. Sansam, P. Tamayo, et al., "Inactivation of the Snf5 Tumor Suppressor Stimulates Cell Cycle Progression and Cooperates With p53 Loss in Oncogenic Transformation," *PNAS* 102, no. 49 (2005): 17745–17750.
30. S. Erkek, P. D. Johann, M. A. Finetti, et al., "Comprehensive Analysis of Chromatin States in Atypical Teratoid/Rhabdoid Tumor Identifies Diverging Roles for SWI/SNF and Polycomb in Gene Regulation," *Cancer Cell* 35, no. 1 (2019): 95–110.e8.

31. T. J. Hulsebos, A. S. Plomp, R. A. Wolterman, E. C. Robanus-Maandag, F. Baas, and P. Wesseling, "Germline Mutation of INI1/SMARCB1 in Familial Schwannomatosis," *American Journal of Human Genetics* 80, no. 4 (2007): 805–810.
32. R. Sestini, C. Bacci, A. Provenzano, M. Genuardi, and L. Papi, "Evidence of a Four-Hit Mechanism Involving SMARCB1 and NF2 in Schwannomatosis-associated Schwannomas," *Human Mutation* 29, no. 2 (2008): 227–231.
33. K. D. Hadfield, W. G. Newman, N. L. Bowers, et al., "Molecular Characterisation of SMARCB1 and NF2 in Familial and Sporadic Schwannomatosis," *Journal of Medical Genetics* 45, no. 6 (2008): 332–339.
34. M. J. Smith, A. J. Wallace, N. L. Bowers, H. Eaton, and D. G. Evans, "SMARCB1 Mutations in Schwannomatosis and Genotype Correlations With Rhabdoid Tumors," *Cancer Genetics* 207, no. 9 (2014): 373–378.
35. T. J. Hulsebos, S. Kenter, W. I. Verhagen, F. Baas, U. Flucke, and P. Wesseling, "Premature Termination of SMARCB1 Translation May be Followed by Reinitiation in Schwannomatosis-Associated Schwannomas, but Results in Absence of SMARCB1 Expression in Rhabdoid Tumors," *Acta Neuropathologica* 128, no. 3 (2014): 439–448.
36. J. J. Swensen, J. Keyser, C. M. Coffin, J. A. Biegel, D. H. Viskochil, and M. S. Williams, "Familial Occurrence of Schwannomas and Malignant Rhabdoid Tumour Associated With a Duplication in SMARCB1," *Journal of Medical Genetics* 46, no. 1 (2009): 68–72.
37. J. Vitte, F. Gao, G. Coppola, A. R. Judkins, and M. Giovannini, "Timing of Smarcb1 and Nf2 Inactivation Determines Schwannoma Versus Rhabdoid Tumor Development," *Nature Communications* 8, no. 1 (2017): 300.
38. S. Avula, A. Peet, G. Morana, et al., "European Society for Paediatric Oncology (SIOPE) MRI Guidelines for Imaging Patients With Central Nervous System Tumours," *Child's Nervous System* 37, no. 8 (2021): 2497–2508.

### Supporting Information

Additional supporting information can be found online in the Supporting Information section.